Colloids and Surfaces B: Biointerfaces 172 (2018) 372–379

Contents lists available at ScienceDirect

Colloids and Surfaces B: Biointerfaces

journal homepage: www.elsevier.com/locate/colsurfb

Comparative studies on amphotericin B nanosuspensions prepared by a high pressure homogenization method and an antisolvent precipitation method

Yixian Zhou[a,1], Qiuyu Fang[b,1], Boyi Niu[a], Biyuan Wu[a], Yiting Zhao[a], Guilan Quan[a,*], Xin Pan[a,*], Chuanbin Wu[a]

[a] School of Pharmaceutical Sciences, Sun Yat-sen University, Guangzhou, 510006, PR China
[b] Shanghai Haohai Biological Technology Co., Ltd., Shanghai, 200052, PR China

ARTICLE INFO

Keywords:
Amphotericin B
Nanosuspensions
High pressure homogenization
Antisolvent precipitation
Solubility
Bioavailability

ABSTRACT

Amphotericin B (AmB) is a widely used polyene antifungal agent; however, its poor solubility limits its clinical application. In this study, AmB nanosuspensions were prepared by a high pressure homogenization method (AmB-HPH) and an antisolvent precipitation method (AmB-AP) to improve the drug solubility. To reveal the distinct influences of these two different preparation methods, systematic comparisons of particle size, crystalline state, wettability, *in vitro* dissolution and *in vivo* pharmacokinetics on the properties of AmB-HPH and AmB-AP were performed. The results indicated that AmB-AP was in an amorphous state, exhibiting higher saturation solubility and dissolution rate than those of AmB-HPH in the crystalline state. However, the relative bioavailability of AmB-HPH was higher than that of AmB-AP *in vivo*, which was likely attributed to its better stability. In conclusion, both AmB-HPH and AmB-AP can enhance the solubility and bioavailability of AmB, but the stability of the nanosuspension prepared by the anti-solvent precipitation method should be carefully considered.

1. Introduction

It was reported that 40% of currently marketed drugs and 75% of the lead compounds in drug discovery are poorly water-soluble [1]. Their low water solubility and poor bioavailability limit their further application in clinical therapy. A growing number of formulation strategies have been developed to solve these problems, including cyclodextrin inclusion complex [2], solid dispersion [3], solid lipid nanoparticles [4], and nanosuspension. Among these, nanosuspension has attracted much attention due to its unique properties, including high drug loading, enhanced stability, low toxicity and improved safety [5]. Nanosuspensions are defined as a colloidal dispersion containing pure drug particles and suitable stabilizers, with a size ranging from 1 to 1000 nm [6]. Smaller particle size increases the specific surface area of particles and decreases the thickness of diffusion boundary layer, resulting in an enhanced dissolution rate [7,8]. Recently, nanosuspensions have been widely used to enhance the solubility and bioavailability of poorly soluble drugs.

The approaches to prepare nanosuspensions can be classified as top-down methods and bottom-up methods [9]. High pressure homogenization technology, as a typical top-down method, can reduce the large size of drug crystals by mechanical abrasion [9]. The antisolvent precipitation method is an effective bottom-up method. In this method, drugs are dissolved in the organic phase and then quickly added to the antisolvent phase. As a result, the drugs precipitate under the supersaturated conditions generated by the solution transfer. The physicochemical properties of nanosuspensions prepared by top-down methods and bottom-up methods were thought to be different due to the different mechanisms involved in these two methods [9,10]. Although nanosuspensions prepared by these two methods have been extensively reported in many studies [11–13], few studies have focused on the distinct influences of preparation methods, which is necessary for the clinical application of nanosuspensions.

Amphotericin B (AmB) is a polyene antifungal agent with a broad antifungal spectrum [14]. It can interact with the sterols on fungal cell membranes and then form channels, resulting in the loss of small molecules and cell death [15]. However, AmB is almost insoluble at a neutral pH (< 1 μg/mL), which leads to insufficient dissolution and poor bioavailability. Recently, various formulation techniques utilizing liposomes [16], nanoparticles [17], and micelles [18] have been developed to enhance the solubility of AmB. However, these formulations were commonly administered by intravenous injection, which had poor

* Corresponding authors at: 132 East Circle at University Town, Guangzhou, 510006, PR China.
E-mail addresses: quanglan@mail.sysu.edu.cn (G. Quan), panxin2@mail.sysu.edu.cn (X. Pan).
[1] These authors made equal contributions to this study.

https://doi.org/10.1016/j.colsurfb.2018.08.016
Received 18 May 2018; Received in revised form 5 August 2018; Accepted 9 August 2018
Available online 10 August 2018
0927-7765/ © 2018 Elsevier B.V. All rights reserved.

compliance and potential acute toxicity. Oral administration exhibits better compliance compared with parenteral administration. Furthermore, it was reported that the oral administration of AmB could effectively reduce nephrotoxicity and hemolysis [19]. It is therefore necessary to develop an ideal formulation of AmB with improved solubility and reduced toxicity for oral administration.

In this study, AmB nanosuspensions were prepared by a high pressure homogenization method and an antisolvent precipitation method to improve the solubility and oral bioavailability of AmB. The effects of process and formulation parameters on the quality of the nanosuspension were investigated. Systematic comparisons of the properties of AmB nanosuspensions prepared by the two different approaches were conducted in terms of particle size distribution, zeta potential, surface morphology, crystalline state, surface wettability, *in vitro* dissolution and *in vivo* pharmacokinetic behaviors.

2. Materials and methods

2.1. Materials

AmB was purchased from North China Pharmaceutical Co., Ltd. (Hebei, China). Polyvinylpyrrolidone K90 (PVP K90) was obtained from Guangzhou Chenqian Co., Ltd. (Guangdong, China). Sodium dodecyl sulfate (SDS) and mannitol were purchased from Tianjin Fuchen Chemical Reagent Co., Ltd. (Tianjin, China). Dimethyl sulfoxide (DMSO) was obtained from Tianjin Fuyu Fine Chemical Co., Ltd. (Tianjin, China). Dialysis bags (molecular weight cut-off: 3500 Da) were purchased from Guangzhou Weijia Technology Co., Ltd. (Guangdong, China). HPLC grade acetonitrile and methanol were purchased from Sinopharm Chemical Reagent Co., Ltd. (Shanghai, China). All other chemicals and solvents were of analytical reagent grade.

Healthy male SD rats (weighing 180–220 g) were purchased from the Experimental Animal Center of Sun Yat-Sen University (Guangdong, China). All of the procedures used in the animal study were approved by the Institutional Animal Care and Use Committee of Sun Yat-sen University in accordance with National Institute of Health and Nutrition Guidelines for the care and use of laboratory animals.

2.2. Preparation of AmB-HPH

First, AmB was dispersed in 50 mL of deionized water at different concentrations (0.3, 0.6, 0.9, 1.2 mg/mL), and the resulting mixture was stirred using a high speed homogenizer (FA25, Shanghai Fluko Co., Ltd., China) at 10,000 rpm for 5 min. The stabilizer PVP K90 was dissolved in 10 mL of deionized water at different concentrations (0.6, 3, 6, 60 mg/mL). Subsequently, the stabilizer solution was rapidly added to the drug solution under stirring, and the obtained coarse suspension was then allowed to homogenize using a high pressure homogenizer with different pressures (500, 800, 1200 bar) and cycles (3, 6, 8, 10, 12, 15). Finally, the nanosuspension was collected after homogenization (Fig. 1).

2.3. Preparation of AmB-AP

Briefly, AmB was dissolved in DMSO at different concentrations (5, 10, 20, 30 or 40 mg/mL) to form the solvent phase. The stabilizers PVP K90 (0.5, 1, 1.5, 2, 5 mg/mL) and SDS (0.2, 0.5, 0.8 mg/mL) were dispersed in deionized water, which was used as the antisolvent phase. Then, the drug solution was added to the antisolvent at a fixed volume ratio of 1:10, 1:20, 1:30, 1:40 and 1:50. DMSO was removed by dialysis against deionized water for 24 h, and the water was replaced at given time intervals (1, 2, 3, 4, 9, 14 and 19 h). Then, the nanosuspension remaining in the dialysis bag was collected (Fig. 1).

2.4. Particle size and zeta potential

The average particle size, polydispersity index (PDI) and zeta potential were determined by dynamic light scattering (DLS) using the Zetasizer (Nano-ZS90, Malvern Instruments Ltd., UK) at 25 ℃. All nanosuspensions were diluted with deionized water by approximately 10 times before measurement to maintain a count rate in the range of 180–250 kcps.

2.5. Particle morphology

Transmission electron microscopy (TEM, JEM-1400, JEOL Ltd., Japan) was used to characterize the surface morphology and dimension. The diluted samples were dropped onto carbon-coated copper grids and stained with phosphotungstic acid (0.1% w/v). After being dried at room temperature, the samples were observed by TEM.

2.6. Solidification of nanosuspensions by freeze drying

A freeze-drying method was used to solidify the nanosuspension for better stability. Briefly, 2 mL of AmB nanosuspension was added to glass vial, followed by addition of mannitol as the cryoprotectant (100 mg). All samples were prefrozen in the refrigerator at −80 °C for 24 h and lyophilized at −50 °C for 48 h using a lyophilizer (Alpha 1–4 LSC, Christ, Germany).

2.7. Powder X-ray diffraction analysis (PXRD)

The crystalline state of samples was analyzed by X-ray diffractometer (D/MAX 2200 VPC, RIGAKU, Japan) at 40 kV and 40 mA with Cu Kα radiation. The samples were scanned from 5–50° (2θ) with a scanning speed rate of 3°/min. The diffraction patterns of AmB, blank excipients (PVP K90 and SDS), physical mixture, optimized AmB-HPH and AmB-AP were recorded.

2.8. Differential scanning calorimetry (DSC)

Thermal properties of AmB, blank excipients (PVP K90 and SDS), physical mixtures, optimized AmB-HPH and AmB-AP were examined using DSC (TGA/SDTA851e, Mettler-Toledo Co., Switzerland). The samples were heated in aluminum pans from 50 °C to 250 °C at a heating rate of 10 °C /min. The measurements were performed under nitrogen flow.

2.9. Contact angle determination

The wettability of AmB, lyophilized AmB-HPH, and AmB-AP was measured using a contact angle meter (JC2000C, Powereach Co., China). Prior to the measurement, 300 mg of sample was dried and compressed to a disk by using a press with a pressure of 10 tons and a duration of 1 min A drop of ultrapure water was placed on the surface of the disk using a micrometer syringe and the contact angle of each drop was determined.

2.10. Saturation solubility and in vitro drug release

An excess amount of AmB, optimized AmB-HPH and AmB-AP was added to 5 mL of distilled water, respectively, and mixed by vortex. Then, the mixtures were stirred for 48 h at 37 ± 0.5 °C to facilitate the equilibrium. The equilibrated samples were centrifuged at 3000 rpm for 5 min. The supernatant was withdrawn, passed through a 0.45 μm filter, and subsequently diluted to a suitable concentration with methanol for quantification of AmB using HPLC.

The *in vitro* release profiles of AmB, optimized AmB-HPH and AmB-AP were performed in a dissolution apparatus (ZRS-8 G, Tianjin University Wireless Factory, China) by the paddle method. Samples

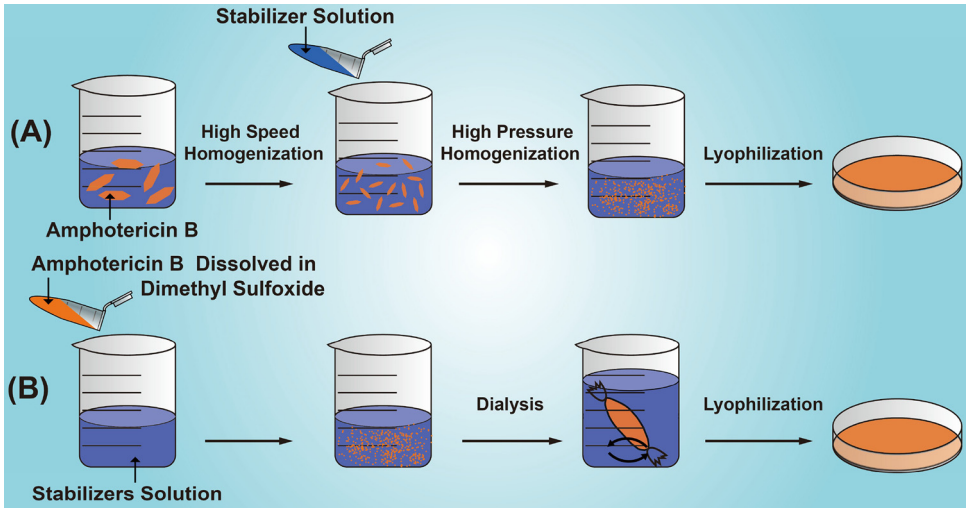

Fig. 1. The schematic preparation of AmB-HPH (A) and AmB-AP (B).

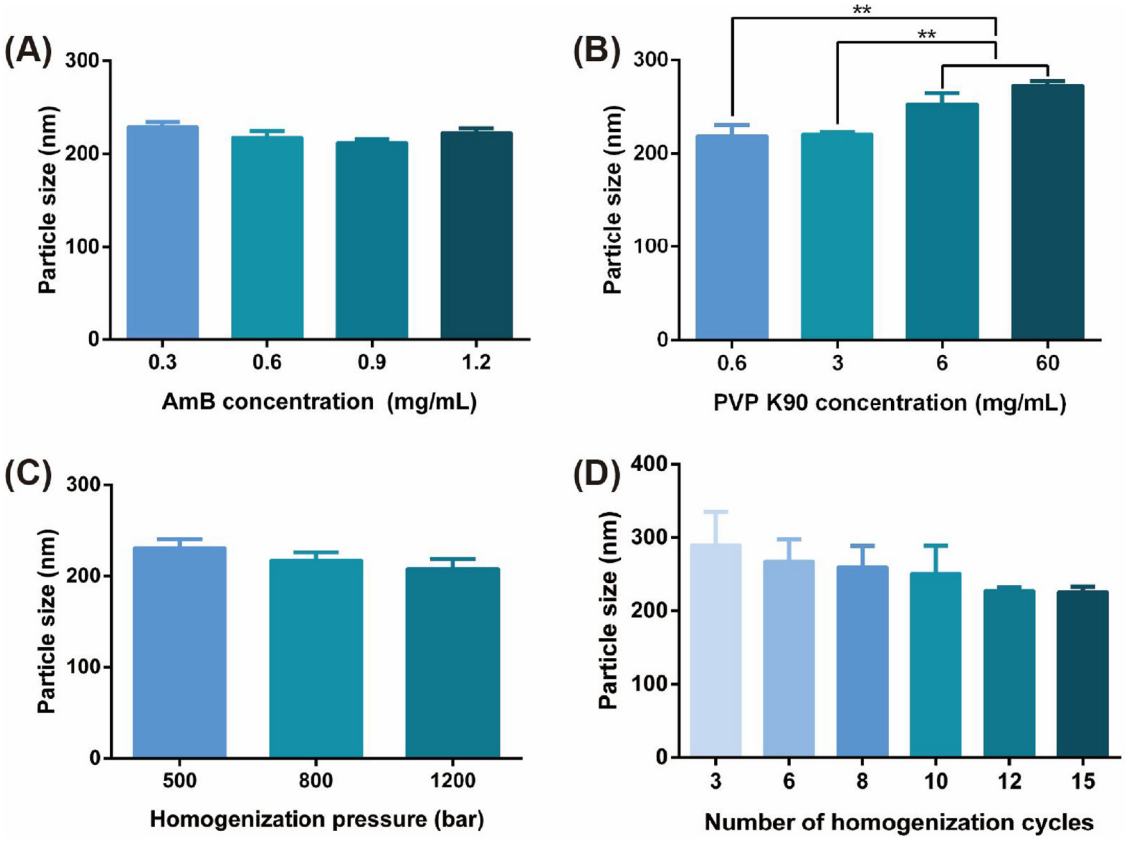

Fig. 2. Particle size of AmB-HPH prepared with different AmB concentrations (A), PVP K90 concentrations (B), homogenization pressures (C) and numbers of homogenization cycles (D) (mean ± S.D., $n = 3$). Significant difference is regarded as $p < 0.05$, * implies $p \leq 0.05$, ** implies $p \leq 0.01$.

containing equivalent amounts of AmB were transferred into 200 mL of phosphate-buffered saline (PBS, pH 7.4) at 37 ± 0.5℃ and stirred at 100 rpm. Aliquot samples (3 mL) were withdrawn at 5, 15, 25, 35, 45 and 60 min and compensated with an equal volume of fresh dissolution medium. Finally, the obtained samples were diluted to a suitable concentration with methanol and assayed by HPLC.

The HPLC system (LC-20, Shimadzu Co., Ltd., Japan) was equipped with an ODS column (Luna 5 μm, 250 × 4.6 mm, Phenomenex). The mobile phase consisted of acetonitrile and water (40:60, v/v) eluted at a flow rate of 1 mL/min. The eluent was monitored at 405 nm and the column temperature was set at 30 ℃. Twenty microliters of sample was injected into the column for measurement.

2.11. In vivo oral pharmacokinetic study

Eighteen male SD rats were randomly divided into three groups (six rats per group). The rats were fasted overnight with free access to water before experiments. Then, the commercial product (sodium deoxycholate micelle of AmB) and the optimized AmB-HPH and AmB-AP were orally administered at a dose of 10 mg/kg. Blood samples were collected from the tail vein into heparinized tubes at 1, 2, 4, 6, 8, 10, 12, and 24 h after administration. The plasma was obtained by

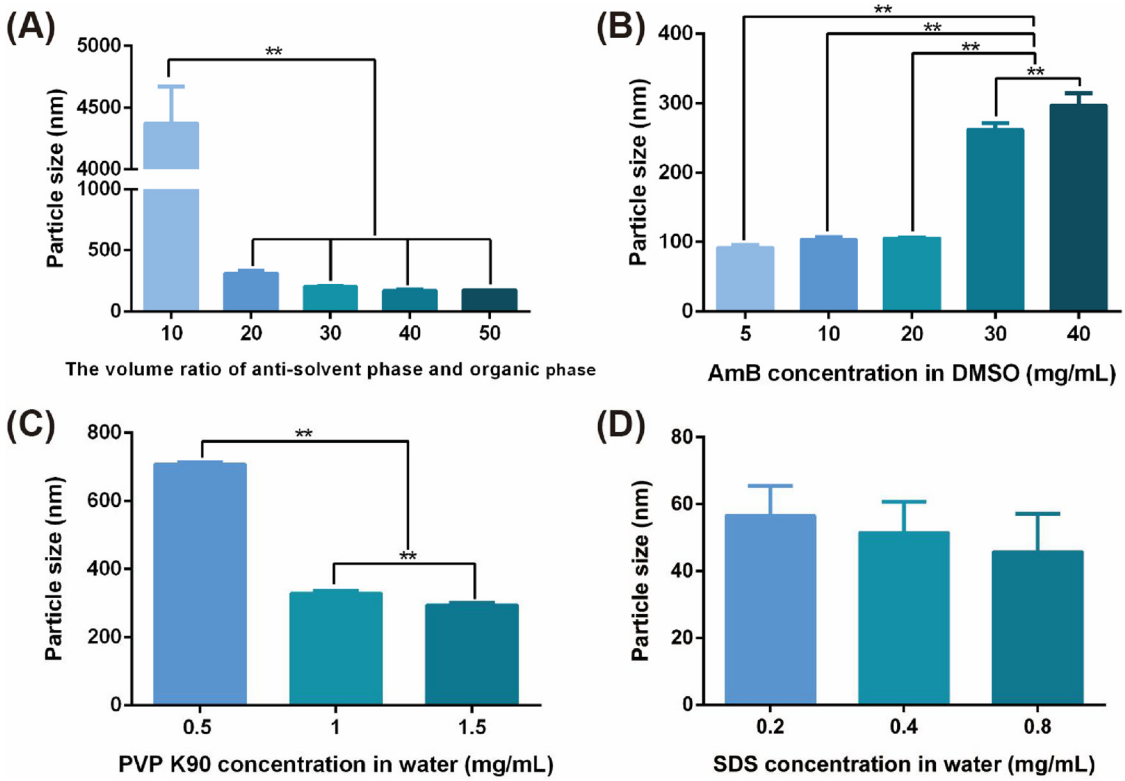

Fig. 3. Particle size of AmB-AP prepared with different volume ratios of antisolvent phase to organic phase (A), AmB concentrations in DMSO (B), PVP K90 concentrations (C) and SDS concentrations (D) (mean ± S.D., $n = 3$). Significant difference is regarded as $p < 0.05$, * implies $p \leq 0.05$, ** implies $p \leq 0.01$.

centrifugation of the blood samples at 3000 rpm for 10 min and then stored at −20 °C for further analysis.

For analysis of drug in plasma, frozen samples were thawed at room temperature and treated as follows. An aliquot (150 μL) of plasma was mixed with 200 μL of methanol and 100 μL of acetonitrile and vortexed for 3 min at room temperature. The mixture was then centrifuged at 16,000 rpm for 15 min to collect 20 μL of supernatant for HPLC analysis. The analysis condition was the same as that described in Section 2.9.

3. Results and discussion

3.1. Preparation of AmB-HPH

High pressure homogenization is a typical top-down method used to prepare nanosuspensions. The coarse suspension was prepared by rapidly adding the stabilizer solution into AmB solution, followed by passing through a high pressure homogenizer. The high velocity of the suspensions in the homogenization gap increased the dynamic pressure, and the static pressure was reduced to below the vapor pressure of water. Hence, water started boiling and vapor bubbles formed. As the suspensions left the homogenization gap, the vapor bubbles drastically imploded, and the drug particle size was ultimately diminished because of the high power of the shockwaves caused by cavitation [9].

The effect of AmB concentration on particle size was studied. As shown in Fig. 2A, no obvious change was observed with drug concentrations ranging from 0.3 to 1.2 mg/mL, which suggested that the drug concentration exhibited negligible influence on particle size. By contrast, increasing the PVP K90 concentration led to a suspension with larger particle size (Fig. 2B). In particular, the particle size of AmB-HPH increased from 219.15 nm to 273.30 nm when the PVP K90 concentration increased from 0.6 mg/mL to 60 mg/mL. These results can be explained as follows. First, PVP K90 coated the particle surface to form a protective layer, which might reduce the shockwaves caused by cavitation. Second, the higher viscosity of the solution with higher PVP K90 concentration could also be responsible for the larger particle size, since the viscous solution would reduce the fluid velocity in the gap and subsequently weaken the power of cavitation.

The homogenization parameter was another important factor determining the particle size of the nanosuspensions. With increasing pressure from 500 to 800 bar, the average particle size of AmB-HPH decreased to approximately 200 nm (Fig. 2C). Higher homogenization pressure enhanced the velocity of the fluid in the gap and reduced the static pressure, which generated more bubbles and provided higher energy to comminute particles [20]. However, no significant change in particle size was observed with the pressure ranging from 800 to 1200 bar. Moreover, higher pressure would cause higher temperature, which might have an adverse effect on the stability of AmB. The number of homogenization cycles might also affect the particle size of AmB-HPH (Fig. 2D). The increasing number of cycles from 3 to 12 led to a size reduction from ~290 nm to ~230 nm. The increased number of cycles provided more energy for comminuting drug particles. However, a further increase in the number of cycles did not result in smaller particle size.

According to the above results, the optimized parameters for AmB-HPH were set as follows. The concentration of AmB was 1.2 mg/mL, the concentration of PVP K90 was 3 mg/mL, the homogenization pressure and the number of cycles were 800 bar and 12, respectively.

3.2. Preparation of AmB-AP

Antisolvent precipitation is an effective method to prepare nanosuspensions. In general, the solvent phase containing dissolved drug was added quickly into the antisolvent phase. Because of the desolvation effect, nanosuspensions formed under supersaturated conditions [10]. The effects of multiple factors on particle size were investigated, including the volume ratio of the antisolvent phase to the organic phase, the concentration of AmB and stabilizers.

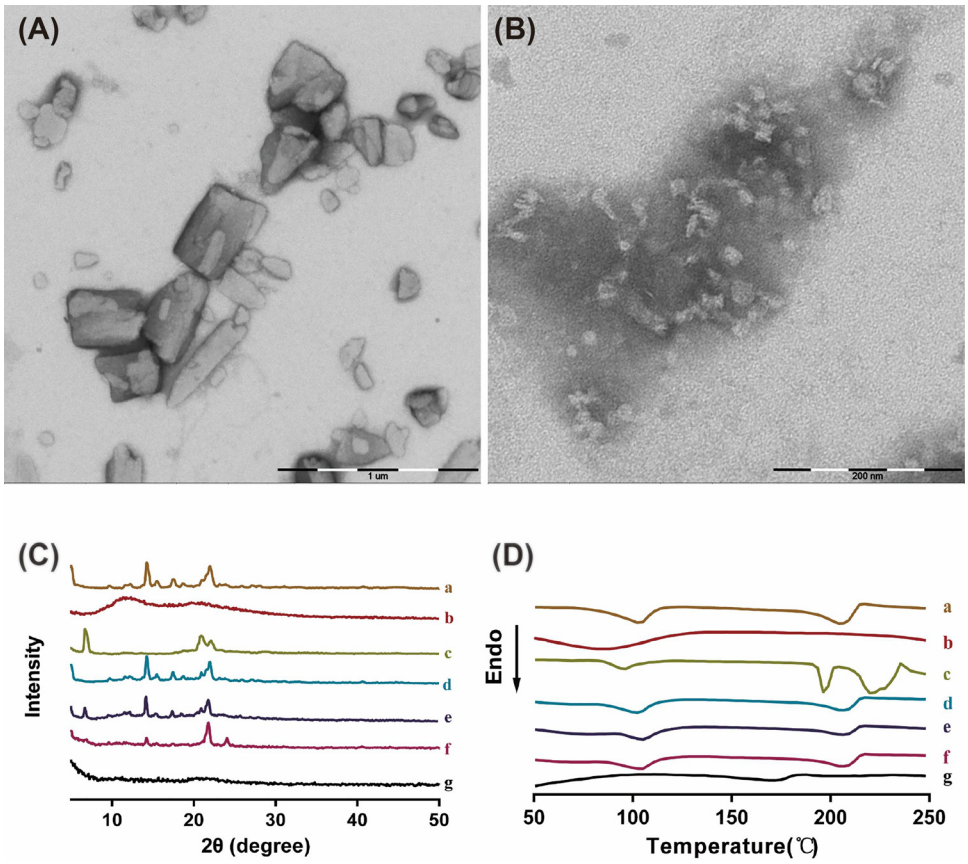

Fig. 4. TEM images of AmB-HPH (A) and AmB-AP (B); (C) PXRD patterns of AmB (a), PVP K90 (b), SDS (c), physical mixture of AmB and PVP K90 (d), physical mixture of AmB, PVP K90 and SDS (e), lyophilized AmB-HPH (f) and lyophilized AmB-AP (g); (D) DSC patterns of AmB (a), PVP K90 (b), SDS (c), physical mixture of AmB and PVP K90 (d), physical mixture of AmB, PVP K90 and SDS (e), lyophilized AmB-HPH (f) and lyophilized AmB-AP (g).

The influence of the volume ratio of the antisolvent phase to the organic phase on the particle size is shown in Fig. 3A. The results showed that the mean particle size of AMB-AP decreased dramatically from a micrometer scale to a nanometer scale when the volume ratio of antisolvent phase to organic phase increased from 10 to 20. The precipitation of AmB from a supersaturated solution normally involves two stages: nucleation and particle growth [21]. A larger volume ratio of antisolvent phase to organic phase would induce higher supersaturation degree of drug solution, leading to the rapid nucleation of drug crystals [20]. This would contribute to form more AmB particles, so the particle size would be reduced. Furthermore, when the volume ratio increased from 20 to 50, the particle size did not show a significant change, indicating that the supersaturation degree might be enough when the volume ratio exceeded 20.

The effect of drug concentration on the particle size of AmB-AP was evaluated and shown in Fig. 3B. The particle size of AmB-AP did not show a significant change when the drug concentration ranged from 5 to 20 mg/mL, but it increased from ~100 nm to ~300 nm when the drug concentration increased from 20 to 40 mg/mL. This behavior could be explained by the change of viscosity [22]. The viscosity of solution would increase with the increasing AmB concentration, which limited the diffusion between the antisolvent phase and the organic phase. As a result, the supersaturated solution was nonuniform, and the particle size became larger. Moreover, higher AmB concentration would increase the probability of particle aggregation, which might also contribute to the larger drug particles.

In this study, the polymer PVP K90 was employed as stabilizer in the AmB-AP preparation, which could be adsorbed on the surface of drug particles to stabilize them by providing steric repulsions. As shown in Fig. 3C, the particle size of AmB-AP decreased with the increase of PVP K90 concentration from 0.5 to 1 mg/mL, demonstrating that PVP K90 inhibited crystal growth and particle aggregation by providing steric repulsions [12]. Moreover, the size of AmB-AP did not obviously decrease as the concentration of PVP K90 changed from 1 to 1.5 mg/mL; therefore, the PVP K90 concentration was set as 1 mg/mL for further studies.

Although PVP K90 stabilized AmB-AP by providing steric repulsions, AmB-AP still aggregated in our previous study. To further improve the stability of AmB-AP, the surfactant SDS was used in AmB-AP preparation. The particle size decreased with the increase of SDS concentration from 0.2 to 0.8 mg/mL (Fig. 3D), indicating that higher SDS concentration favored smaller particle size. The concentration of SDS was set as 0.2 mg/mL in further studies to minimize unwanted side effects.

Therefore, the optimal conditions for AmB-AP were set as follows. The volume ratio of antisolvent phase to organic phase was 20, the AmB concentration was 20 mg/mL, the concentration of PVP K90 and SDS was 1 mg/mL and 0.2 mg/mL, respectively.

3.3. Characterization of optimized AmB-HPH and AmB-AP

3.3.1. Particle size, zeta potential and morphology

The average particle sizes of the optimized AmB-HPH and AmB-AP were 227.86 ± 4.14 nm and 56.66 ± 8.77 nm, respectively. PDI indicates the uniformity of size distribution, which is an important factor determining the stability of nanosuspension. A higher PDI value represents a broader size distribution, which may facilitate Ostwald ripening, eventually resulting in particle growth and aggregation [23]. Generally, a PDI value under 0.3 indicates a good uniformity. In this study, the PDI values of AmB-HPH and AmB-AP were 0.132 ± 0.025 and 0.299 ± 0.013, respectively. The comparatively narrow particle size distribution indicated good uniformity of the prepared particles. Zeta potential is also an essential factor of the stability of colloidal dispersions. Generally, a zeta potential below −20 mV was sufficient to stabilize the nanosuspension [24]. In this study, the zeta potentials of the optimized AmB-HPH and AmB-AP were −22.4 ± 2.26 mV and

−26.87 ± 2.54 mV, respectively, demonstrating that these both nanosupensions were theoretically stable.

The morphologies of the optimized AmB-HPH and AmB-AP were observed using TEM. Fig. 4A shows that AmB-HPH appeared as an irregular shape, which might be attributed to the shockwaves of high pressure homogenization and the high hardness of drug particles. AmB-AP (Fig. 4B) was spherical in appearance with uniform size distribution, which might be attributed to the precipitation process. In addition, the particle size obtained by TEM was approximately 40 nm, which was smaller than that obtained by DLS due to the existence of solvation layers in the DLS analysis [25].

3.3.2. PXRD analysis

PXRD was used to characterize the crystalline states of samples. The PXRD patterns of AmB, PVP K90, SDS, physical mixtures, and lyophilized AmB-HPH and AmB-AP are illustrated in Fig. 4C. The X-ray pattern of AmB displayed intense peaks at 2θ of 14.6° and 21.7°, indicating its crystalline structure. The X-ray pattern of PVP K90 did not show any characteristic peaks because of its amorphous nature. The physical mixtures showed a similar X-ray pattern to that of AmB, suggesting that the excipients would not influence the crystalline structure of AmB. The characteristic peaks of AmB were also observed in lyophilized AmB-HPH, indicating that the crystalline state of AmB had no obvious change during the high pressure homogenization process. However, the characteristic peaks of AmB were not observed for lyophilized AmB-AP, suggesting the transition of AmB from the crystalline state to the amorphous state during the precipitation.

3.3.3. DSC analysis

DSC analysis was performed to further confirm the physical state of various samples. As shown in Fig. 4D, AmB and the physical mixtures exhibited endothermic melting peaks at 107 °C and 204.5 °C due to the existence of crystalline drug. In addition, the characteristic endothermic peaks of AmB were also observed in lyophilized AmB-HPH. However, no characteristic peaks of AmB were detected in the thermogram of freeze-dried AmB-AP, confirming the absence of any crystalline phase of AmB during the precipitation. These results were consistent with the results of PXRD.

3.3.4. Contact angle

Surface wettability of a solid can be evaluated by the contact angle between the perimeter of a water drop and the surface [26,27]. A large contact angle typically indicates poor surface wettability. As shown in Fig. 5, the contact angle of AmB was 50°, while the contact angles of lyophilized AmB-HPH and AmB-AP were reduced to 32° and 16°, respectively. This demonstrated that both the high pressure homogenization method and antisolvent precipitation method remarkably improved the poor surface wettability of AmB by reducing the particle size. Moreover, the surface wettability of AmB-AP was superior to that of AmB-HPH, which might be attributed to the reduced particle size and amorphous state of AmB-AP. In addition, the distinct morphological properties of AmB-HPH and AmB-AP might also affect their surface wettability [13].

3.4. Saturation solubility and in vitro dissolution

Freeze-dried powders of the optimized nanosuspensions were prepared to measure the saturation solubility. The particle sizes of redispersed suspensions of lyophilized AmB-HPH and AmB-AP were 211.4 nm and 68.2 nm, respectively, which was similar to the original nanosuspension. The saturation solubility of AmB, lyophilized AmB-HPH and AmB-AP was 0.22 ± 0.01, 27.53 ± 2.78 and 281.64 ± 1.25 μg/mL, respectively. The solubility of AmB-HPH and AmB-AP was significantly higher than that of AmB, indicating that both high pressure homogenization and antisolvent precipitation were effective approaches to improve the solubility of AmB. In addition, the saturation solubility of AmB-AP was more than ten times higher than that of AmB-HPH, which would be mainly ascribed to the reduction in particle size and the difference in crystalline state. According to the Noyes-Whitney equation, the relatively smaller particle size of AmB-AP would lead increased solubility [28]. Furthermore, according to the data of PXRD and DSC, AmB-HPH was in a crystalline state, whereas AmB-AP was in an amorphous form. With lower lattice energy, the amorphous state of AmB-AP also contributed to improved surface wettability, eventually leading to enhanced solubility. Moreover, the additional stabilizer, SDS, may further improve the solubility of AmB-AP by forming micelles.

AmB is weakly acidic and hardly soluble in simulated gastric fluid (pH 1.2) [29]. Therefore, the *in vitro* drug release assay was conducted in PBS buffer (pH 7.4). The dissolution profiles of AmB, lyophilized AmB-HPH and AmB-AP are presented in Fig. 6A. The release rate of AmB in PBS was quite low, and only approximately 0.5% of drug was released within 60 min. In contrast, approximately 90% of AmB released from AmB-AP in 5 min, and complete release was realized at 15 min. However, lyophilized AmB-HPH did not achieve complete dissolution and only about 70% of drug was released in 60 min. These results were consistent with the results of saturation solubility. The differences in dissolution profiles between lyophilized AmB-HPH and AmB-AP can be explained by the following reasons. First, compared with AmB-HPH, the smaller particle size of AmB-AP increased the surface available for dissolution and decreased the thickness of the diffusion layer [30]. Second, the amorphous state of AmB-AP with high energy led to the improvement of the dissolution rate [31,32]. Furthermore, SDS may further improve the dissolution rate of AmB-AP.

3.5. Pharmacokinetic study

The HPLC method for quantitative determination of AmB in rat plasma was validated before the pharmacokinetic study. The calibration curve of AmB in plasma was linear in the range from 0.107 to 1.72 μg/mL. The relative standard deviation (RSD) values of intra- and interday precision at three different concentrations (0.26, 0.52 and 1.04 μg/mL) were 3.73%, 0.63%, 4.35%, 8.87%, 8.71% and 2.55%, which were all below 10%. These results demonstrated that the constructed HPLC method for determining the AmB concentration in plasma had good sensitivity and reproducibility.

In this study, the pharmacokinetic profiles of AmB-HPH, AmB-AP

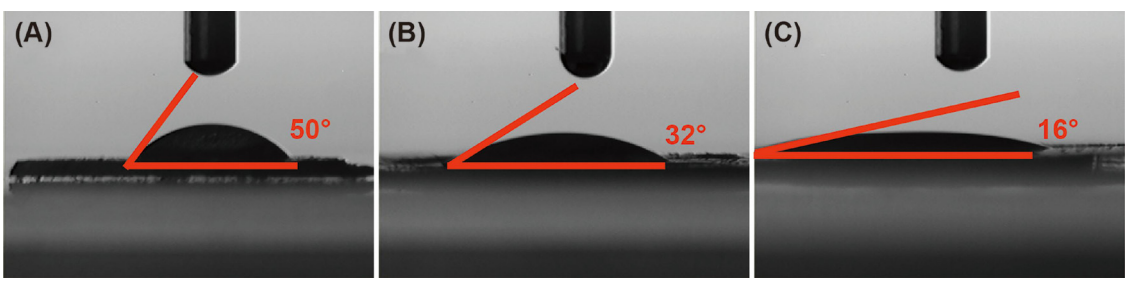

Fig. 5. Contact angles of AmB (A), lyophilized AmB-HPH (B) and lyophilized AmB-AP (C).

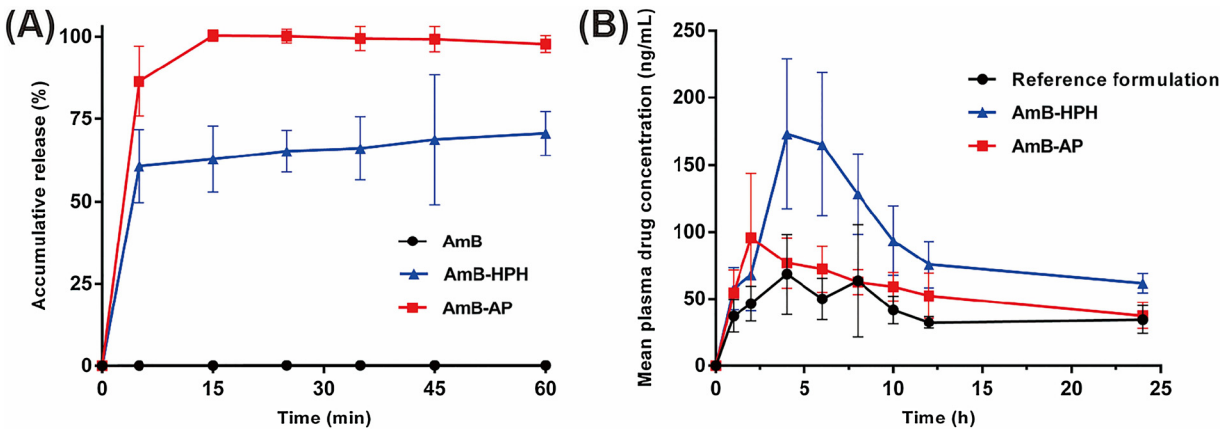

Fig. 6. (A) Release curves of AmB, AmB-HPH and AmB-AP in PBS (pH 7.4) (mean ± S.D., $n = 3$); (B) Plasma concentration-time curves after oral administration of reference formulation (sodium deoxycholate micelle of AmB), AmB-HPH and AmB-AP to rats at a dose of 10 mg/kg (mean ± S.D., $n = 6$).

and sodium deoxycholate micelle of AmB (the reference formulation) are shown in Fig. 6B. The plasma concentrations of AmB after oral administration of AmB-HPH and AmB-AP were higher than that of the reference formulation during the tested time, indicating that both the high pressure homogenization and antisolvent precipitation methods were effective in increasing the plasma concentration of AmB. Furthermore, the drug concentration of AmB-HPH was much higher than that of AmB-AP at nearly each time point, especially the middle time points.

To make a further comparison, the main pharmacokinetic parameters were calculated and are presented in Table 1. The two-compartment model was the best fit for all three groups. The maximum drug concentrations in plasma (C_{max}) of AmB-HPH and AmB-AP were 2.69 times and 1.48 times higher than that of the reference formulation, respectively. Moreover, the area under the curve (AUC_{0-t}) values of the reference formulation, AmB-HPH and AmB-AP were 822.09, 2178.03 and 1262.69 ng h/mL, respectively. The relative bioavailability of AmB-HPH and AmB-AP was 264.94% and 153.60% in comparison to the reference formulation, demonstrating that the oral bioavailability of AmB can be enhanced by formulating the drugs into nanosuspensions.

It is noteworthy that AmB-HPH had higher plasma concentration, C_{max} value and relative bioavailability compared with AmB-AP, which was inconsistent with the surface wettability, saturation solubility and dissolution results. This might be attributed to the amorphous state of AmB-AP, which was unstable and liable to recrystallize, ultimately led to the decreased oral bioavailability [9]. To confirm this hypothesis, lyophilized AmB-HPH and AmB-AP were separately dispersed in simulated gastric fluid (SGF) for 4 h to evaluate the stability. The results showed that there was no distinct change in the particle size of AmB-HPH, while the lyophilized AmB-AP with additional ionic stabilizer, SDS, aggregated and precipitated rapidly in SGF. The instability of AmB-AP can be mainly ascribed to the thermodynamically unstable solution generated by AmB-AP. A supersaturated solution exceeding the equilibrium solubility will be formed after fast dissolution of amorphous drug. Theoretically, drug at high concentration has an increased driving force for oral absorption. However, supersaturated drug with higher energy tends to precipitate rapidly into the energetically favorable crystalline state. Moreover, the PDI value of AmB-AP was higher than that of AmB-HPH, which may facilitate Ostwald ripening, subsequently accelerating the particle growth and increasing the particle size. AmB-AP (~250 nm) can cross the intestinal membranes and enter blood circulation easily, while aggregated AmB-HPH may be hard to interact with the intestinal membranes and enter blood circulation [33,34]. The precipitation effect of AmB-AP ultimately led to compromised bioavailability. Hence, the stability of nanosuspension in SGF should be carefully considered when a nanosuspension formulation is prepared by an antisolvent precipitation method.

4. Conclusion

In this study, AmB nanosuspensions were successfully prepared by the high pressure homogenization method and antisolvent precipitation method. AmB-HPH appeared as irregular shape with a particle size of approximately 200 nm, while AmB-AP appeared as spherical particles with a particle size of approximately 60 nm. The results of PXRD and DSC demonstrated that AmB-HPH and AmB-AP were in a crystalline state and amorphous state, respectively. Moreover, the saturation solubility and dissolution of AmB-AP were superior to those of AmB-HPH due to its smaller particle size and amorphous state. However, AmB-HPH exhibited higher relative bioavailability than AmB-AP due to its better stability, while both were superior in bioavailability in comparison with the commercial product. Overall, the comparative studies between AmB-HPH and AmB-AP have been investigated. However, further extensive investigation concerning the long term stability and the relevant mechanism is required.

Acknowledgements

The authors appreciate financial support from the National Natural Science Foundation of China (81773660), the Natural Science Fund

Table 1
Pharmacokinetic parameters after oral administration of the reference formulation (sodium deoxycholate micelles of AmB), AmB-HPH and AmB-AP to rats at a dose of 10 mg/kg; each value represents the mean ± S.D. ($n = 6$).

Parameters	Reference formulation	AmB-HPH	AmB-AP
T_{max} (h)	5.00 ± 1.67	5.30 ± 1.63	4.33 ± 2.34
C_{max} (ng/ml)	73.58 ± 22.79	198.71 ± 34.57**	108.88 ± 38.92
AUC_{0-24h} (ng h/ml)	822.09 ± 222.80	2178.03 ± 107.72**	1262.69 ± 181.75**
MRT_{0-24h} (h)	9.46 ± 2.90	10.46 ± 0.28	9.72 ± 2.36

Statistical analysis was performed by unpaired '*t*' test using Graphpad Prism 6.02 software. Significant difference is regarded as $p < 0.05$, * implies $p \leq 0.05$, ** implies $p \leq 0.01$ as compared to the reference formulation.

Project of Guangdong Province (2016A030312013), the Science and Technology Foundation of Nansha District (2016KF012), and 111 project (B16047).

References

[1] H.D. Williams, N.L. Trevaskis, S.A. Charman, R.M. Shanker, W.N. Charman, C.W. Pouton, et al., Strategies to address low drug solubility in discovery and development, Pharmacol. Rev. 65 (2013) 315–499.

[2] Z.I. Yildiz, A. Celebioglu, T. Uyar, Polymer-free electrospun nanofibers from sulfobutyl ether(7)-beta-cyclodextrin (SBE7-beta-CD) inclusion complex with sulfisoxazole: fast-dissolving and enhanced water-solubility of sulfisoxazole, Int. J. Pharm. 531 (2017) 550–558.

[3] A. Singh, G. Van den Mooter, Spray drying formulation of amorphous solid dispersions, Adv. Drug Deliv. Rev. 100 (2016) 27–50.

[4] S. Doktorovova, A.B. Kovacevic, M.L. Garcia, E.B. Souto, Preclinical safety of solid lipid nanoparticles and nanostructured lipid carriers: current evidence from in vitro and in vivo evaluation, Eur. J. Pharm. Biopharm. 108 (2016) 235–252.

[5] R.H. Muller, S. Gohla, C.M. Keck, State of the art of nanocrystals - Special features, production, nanotoxicology aspects and intracellular delivery, Eur. J. Pharm. Biopharm. 78 (2011) 1–9.

[6] Y.C. Wang, Y. Zheng, L. Zhang, Q.W. Wang, D.R. Zhang, Stability of nanosuspensions in drug delivery, J. Control. Release 172 (2013) 1126–1141.

[7] L.B. Wu, J. Zhang, W. Watanabe, Physical and chemical stability of drug nanoparticles, Adv. Drug Deliv. Rev. 63 (2011) 456–469.

[8] M. Mosharraf, C. Nystrom, The effect of particle size and shape and the surface specific dissolution rate of microsized practically insoluble drugs, Int. J. Pharm. (Amsterdam) 122 (1995) 35–47.

[9] R. Shegokar, R.H. Muller, Nanocrystals: industrially feasible multifunctional formulation technology for poorly soluble actives, Int. J. Pharm. 399 (2010) 129–139.

[10] J. Du, X.G. Li, H.X. Zhao, Y.Q. Zhou, L.L. Wang, S.S. Tian, et al., Nanosuspensions of poorly water-soluble drugs prepared by bottom-up technologies, Int. J. Pharm. 495 (2015) 738–749.

[11] L.G. Guo, L. Kang, X.R. Liu, X.Y. Lin, Wu Y. Di DH, et al., A novel nanosuspension of andrographolide: preparation, characterization and passive liver target evaluation in rats, Eur. J. Pharm. Sci. 104 (2017) 13–22.

[12] B.K. Ahuja, S.K. Jena, S.K. Paidi, S. Bagri, S. Suresh, Formulation, optimization and in vitro-in vivo evaluation of febuxostat nanosuspension, Int. J. Pharm. 478 (2015) 540–552.

[13] T.T.D. Tran, P.H.L. Tran, M.N.U. Nguyen, K.T.M. Tran, M.N. Pham, P.C. Tran, et al., Amorphous isradipine nanosuspension by the sonoprecipitation method, Int. J. Pharm. 474 (2014) 146–150.

[14] S. Campoy, J.L. Adrio, Antifungals, Biochem. Pharmacol. 133 (2017) 86–96.

[15] P. Caffrey, S. Lynch, E. Flood, S. Finnan, M. Oliynyk, Amphotericin biosynthesis in Streptomyces nodosus: deductions from analysis of polyketide synthase and late genes, Chem. Biol. 8 (2001) 713–723.

[16] R. Hamill, Amphotericin B formulations: a comparative review of efficacy and toxicity, Drugs 73 (2013) 919–934.

[17] H. Zazo, C.I. Colino, J.M. Lanao, Current applications of nanoparticles in infectious diseases, J. Control. Release 224 (2016) 86–102.

[18] M.C. Branco, J.P. Schneider, Self-assembling materials for therapeutic delivery, Acta Biomater. 5 (2009) 817–831.

[19] J.J. Torrado, R. Espada, M.P. Ballesteros, S. Torrado-Santiago, Amphotericin B formulations and drug targeting, J. Pharm. Sci. 97 (2008) 2405–2425.

[20] L. Gao, D.R. Zhang, M.H. Chen, Drug nanocrystals for the formulation of poorly soluble drugs and its application as a potential drug delivery system, J. Nanoparticle Res. 10 (2008) 845–862.

[21] H.K. Chan, P.C.L. Kwok, Production methods for nanodrug particles using the bottom-up approach, Adv. Drug Deliv. Rev. 63 (2011) 406–416.

[22] J.Y. Zhang, Z.G. Shen, J. Zhong, T.T. Hu, J.F. Chen, Z.Q. Ma, et al., Preparation of amorphous cefuroxime axetil nanoparticles by controlled nanoprecipitation method without surfactants, Int. J. Pharm. 323 (2006) 153–160.

[23] L.L. Zong, X.H. Li, H.Y. Wang, Y.P. Cao, L. Yin, M.M. Li, et al., Formulation and characterization of biocompatible and stable IV itraconazole nanosuspensions stabilized by a new stabilizer polyethylene glycol-poly(beta-Benzyl-L-aspartate) (PEG-PBLA), Int. J. Pharm. 531 (2017) 108–117.

[24] Y. Liang, J. Binner, Effect of triblock copolymer non-ionic surfactants on the rheology of 3 mol% yttria stabilised zirconia nanosuspensions, Ceram. Int. 34 (2008) 293–297.

[25] P. Pei, F. Yang, J. Liu, H. Hu, X. Du, N. Hanagata, et al., Composite-dissolving microneedle patches for chemotherapy and photothermal therapy in superficial tumor treatment, Biomater. Sci. 6 (6) (2018) 1414–1423.

[26] J.T. Korhonen, T. Huhtamaki, O. Ikkala, R.H.A. Ras, Reliable measurement of the receding contact angle, Langmuir 29 (2013) 3858–3863.

[27] J. Pardeike, R.H. Mueller, Nanosuspensions: a promising formulation for the new phospholipase A(2) inhibitor PX-18, Int. J. Pharm. 391 (2010) 322–329.

[28] R.H. Muller, C.M. Keck, Challenges and solutions for the delivery of biotech drugs - a review of drug nanocrystal technology and lipid nanoparticles, J. Biotechnol. 113 (2004) 151–170.

[29] B. Amarji, Ajazuddin, D. Raghmanshi, S.P. Vyas, P. Kanaujia, Lipid Nano Spheres (LNSs) for enhanced oral Bioavailability of amphotericin B: development and characterization, J. Biomed. Nanotechnol. 3 (2007) 264–269.

[30] C. Hong, Y. Dang, G. Lin, Y. Yao, G. Li, G. Ji, et al., Effects of stabilizing agents on the development of myricetin nanosuspension and its characterization: an in vitro and in vivo evaluation, Int. J. Pharm. 477 (2014) 251–260.

[31] F. Kesisoglou, S. Panmai, Y.H. Wu, Nanosizing - oral formulation development and biopharmaceutical evaluation, Adv. Drug Deliv. Rev. 59 (2007) 631–644.

[32] B.C. Hancock, M. Parks, What is the true solubility advantage for amorphous pharmaceuticals? Pharm. Res. 17 (2000) 397–404.

[33] F. Xia, W.F. Fan, S.F. Jiang, Y.H. Ma, Y. Lu, J.P. Qi, et al., Size-dependent translocation of nanoemulsions via oral delivery, ACS Appl. Mater. Interfaces 9 (2017) 21660–21672.

[34] Y. Xie, B. Shi, F. Xia, J. Qi, X. Dong, W. Zhao, et al., Epithelia transmembrane transport of orally administered ultrafine drug particles evidenced by environment sensitive fluorophores in cellular and animal studies, J. Control. Release 270 (2018) 65–75.